Petroleum Science (2018) 15:870–881
https://doi.org/10.1007/s12182-018-0268-4

ORIGINAL PAPER

Amorphous TiO_2-supported Keggin-type ionic liquid catalyst catalytic oxidation of dibenzothiophene in diesel

Zhendong Yu[1] · Donghui Wang[1] · Suhang Xun[2] · Minqiang He[1] · Ruliang Ma[1] · Wei Jiang[3] · Hongping Li[3] · Wenshuai Zhu[1] · Huaming Li[3]

Received: 14 April 2018 / Published online: 20 October 2018

Abstract
Supported ionic liquid (IL) catalysts $[C_n mim]_3PMo_{12}O_{40}$/Am TiO_2 (amorphous TiO_2) were synthesized through a one-step method for extraction coupled catalytic oxidative desulfurization (ECODS) system. Characterizations such as FTIR, DRS, wide-angle XRD, N_2 adsorption–desorption and XPS were applied to analyze the morphology and Keggin structure of the catalysts. In ECODS with hydrogen peroxide as the oxidant, it was found that ILs with longer alkyl chains in the cationic moiety had a better effect on the removal of dibenzothiophene. The desulfurization could reach 100% under optimal conditions, and GC–MS analysis was employed to detect the oxidized product after the reaction. Factors affecting the desulfurization efficiencies were discussed, and a possible mechanism was proposed. In addition, cyclic experiments were also conducted to investigate the recyclability of the supported catalyst. The catalytic activity of $[C_{16}mim]_3PMo_{12}O_{40}$/Am TiO_2 only dropped from 100% to 92.9% after ten cycles, demonstrating the good recycling performance of the catalyst and its potential industrial application.

Keywords Supported ionic liquid catalyst · Polyoxometallate · Oxidative desulfurization · Amorphous TiO_2 · Dibenzothiophene

1 Introduction

Nowadays, environmental problems due to the annually increasing emission of sulfur oxides (SO_x) have aroused worldwide attention (Piccinino et al. 2017; Zeng et al. 2017). The main cause of SO_x release is the combustion of sulfur-containing fuels. To handle this, ultralow-sulfur and even sulfur-free fuels are necessary (Li et al. 2009; Xun et al. 2015; Rafiee et al. 2016). Standard regulations for ultralow-sulfur diesel oil (less than 10 ppm) are formulated by governments and multinational organizations (Zheng et al. 2013; Khodayari and Odenbrand 2001; Guldhe et al. 2017). Most available low-sulfur crude reservoirs in nature have been depleted, so it is a big challenge to remove the sulfur content from diesel oil (Dai et al. 2017). Hydrodesulfurization (HDS) is the most wide-range industrialized application in this domain (Liu et al. 2017; Yang et al. 2017). However, the high energy consumption, usually under conditions of 300–400 °C and 20–130 atm (Ibrahim et al. 2017), and the low aromatic sulfur removal rate are problems. To further eliminate aromatic sulfides, such as dibenzothiophene (DBT) and its derivatives, more severe conditions must be employed by refiners which definitely escalates the cost (Jiang et al. 2016). In addition to the HDS method, biodesulfurization (BDS), adsorptive desulfurization (ADS), extractive desulfurization (EDS) and oxidative desulfurization (ODS) have also been widely studied. BDS (Alejandro Dinamarca et al. 2014) is a low energy-consuming technology; sulfur contents in the oil

Edited by Xiu-Qin Zhu

Handling editor: Wenshuai Zhu

✉ Minqiang He
hemq@ujs.edu.cn

✉ Huaming Li
lhm@ujs.edu.cn

[1] School of Chemistry and Chemical Engineering, Jiangsu University, Zhenjiang 212013, People's Republic of China

[2] School of Environment and Safety Engineering, Institute of Environmental Health and Ecological Security, Jiangsu University, Zhenjiang 212013, People's Republic of China

[3] Institute for Energy Research, Jiangsu University, Zhenjiang 212013, People's Republic of China

phase can be reduced by isolated microorganisms. But compared with the chemical process, the BDS reaction time is much longer and the consumption of microorganisms is also high; additionally, the tougher conditions to maintain microorganisms alive limit the application in industry. Without H_2S emission, different kinds of porous adsorbents are employed to eliminate sulfur compounds in ADS systems (Selvavathi et al. 2009; Srivastav and Srivastava 2009). These include alumina, carbon-based materials, zeolites, metal organic frameworks (MOFs) (Ahmed et al. 2017; Bhadra et al. 2017; Khan and Jhung 2017) and so on. At low temperatures, though no hydrogen is needed for the ADS procedure, the ADS selective activity for specific sulfides still needs to be further developed. In spite of mild conditions, sulfur compounds in diesel oil can be reduced by EDS (Nan et al. 2008; Nejad and Beigi 2015) but without catalysts, the single extractive desulfurization performance is still poor and multiple extraction steps are necessary. Oxidative desulfurization (ODS) (Chica et al. 2006; Otsuki et al. 2000; Wang et al. 2003; Jiang et al. 2014) is one of the most promising means in sulfur removal, especially suitable for oxidation of aromatic sulfides like benzothiophene (BT), DBT and so on. ODS provides an efficient and green method for converting sulfides into corresponding sulfones with high selectivity (Zhang et al. 2017b; Li et al. 2016). Based on ODS and EDS processes, a combined system extractive coupled oxidative desulfurization (ECODS) is proposed.

Ionic liquids (ILs) are widely applied in various fields due to their non-flammability, high ionic conductivity, wide electrochemical window and good thermal stability (Ibrahim et al. 2017; Domanska and Wlazlo 2014). Besides, different kinds of ionic liquids can also be specially designed for functional morphology and structure. Hydrophilicity and hydrophobicity are one of the most important parameters of ionic liquids, and these properties can be controlled by changing the length of the carbon chain. In this work, the effects of hydrophilicity and hydrophobicity for desulfurization will be researched carefully. ILs can also be used as catalysts and extractants in desulfurization (Jiang et al. 2017; Zhang et al. Zhang et al. 2017a, 2018; Moghadam et al. 2017; Song et al. 2017). But the separation of ionic liquids in a homogeneous reaction system and subsequent cycle experiments is hard to achieve (Pham et al. 2018; Khan et al. 2018). For further applications, it is necessary to achieve a heterogeneous reaction system by loading the IL on a suitable support. In the oil phase, the dispersion and catalytic activity of the catalyst are significantly affected by the characteristics of the carrier during the sulfur removal process. These include hydrophilic or hydrophobic properties, hole parameters, structure and composition. TiO_2 is one of the supports with excellent performance and widely applied in the field of catalysis. Intensive research has demonstrated favorable interactive effects and stability between catalysts and TiO_2 support (Kim et al. 2013; Morales-Ortuño et al. 2016; Vozka et al. 2017; Morales-Ortuño and Klimova 2017).

Compared to the homogeneous desulfurization system, heterogeneous desulfurization system has more advantages. In homogeneous desulfurization, the excess use of ionic liquid acting as the catalyst for high desulfurization rates may contribute to an increase in cost (Elwan et al. 2017; Rodríguez-Cabo et al. 2014). But when the ionic liquid was supported on a carrier first and then participated in ODS, the same performance could be easily achieved with less ionic liquid in the formed heterogeneous system (Pham et al. 2018; Khan et al. 2018). Besides, the mechanism of the main reaction and possible side reaction in the heterogeneous system can be investigated with convenience (Xun et al. 2016). Moreover, it facilitates catalyst recovery and recycling by simply drying after the reaction. And the high selection of oxidative activity on target aromatic sulfides in the system promotes the oxidation and separation processes (Zhang et al. 2014b).

It is well known that polyoxometalates have good catalytic activity (Yao et al. 2016; Zhang et al. 2016; Gao et al. 2018). According to structure, they can be categorized as Keggin, Dawson, Anderson, Waugh or Silverton types and so on (Alsalme et al. 2016). In this work, supported IL catalysts $[C_n\text{mim}]_3PMo_{12}O_{40}$/Am TiO_2 (n = 4, 8, 16) with Keggin structure were prepared and investigated in ECODS. The systematic studies demonstrate the extractant and the oxidant play key roles in deep sulfur removal in ECODS. Meanwhile, characterizations, TG, FTIR, DRS, XRD, BET and XPS, were applied to verify the successful loading and structure of catalysts. Comprehensively, $[C_{16}\text{mim}]_3PMo_{12}O_{40}$/Am TiO_2 has the optimal desulfurization rate and recycling performance in heterogeneous reaction.

2 Experimental

2.1 Materials

Benzothiophene (BT, 99%) and dibenzothiophene (DBT, 98%) were obtained from Sigma-Aldrich Corporation. 3-Methylbenzothiophene (3-MBT, 96%), 4-methyldibenzothiophene (4-MDBT, 96%), n-tetradecane (99%) and tetrabutyl titanate (99%) were purchased from Aladdin Industrial Corporation. Commercially available H_2O_2 (aqueous solution, 30%), phosphomolybdic acid $H_3PMo_{12}O_{40}$ (AR grade), n-octane (CP grade), acetone (AR grade), ethanol (AR grade) and acetonitrile (AR grade) were from Sinopharm Chemical Reagent Co., Ltd. (China). All of the ionic liquids used in this work were purchased

from Shanghai Chengjie Chemical Co., Ltd. (China) and used without extra purification, as were the other reagents.

2.2 Catalyst preparation

By means of a one-step method, a series of TiO_2-supported Keggin structure-containing ionic liquids were prepared ($[C_n mim]_3PMo_{12}O_{40}$ is abbreviated as C_nPMo), for example, as C_{16}PMo-TiO_2. Typically, 5 mmol $H_3PMo_{12}O_{40}$ and 15 mmol $[C_{16}mim]Cl$ were employed to prepare C_{16}PMo IL. Then, 0.2080 g C_{16}PMo was added in 5 mL acetonitrile, with even stirring at a temperature of 50 °C in an oil bath until no bulk compounds could be observed. A certain amount of tetrabutyl titanate and 0.52 mL of ammonia was added to the dispersion, and the mixture was kept stirring for 3 h. Subsequently, all the mixed solution was transferred into a Teflon-lined autoclave and hydrothermally crystallized at 100 °C for 24 h. The colloid obtained after crystallization was suction-filtered and washed several times and then dried at 120 °C for 3 h. The resulting solid was put in a muffle furnace for 180 min heating at 250 °C in air and then cooled to room temperature to obtain a supported ionic liquid catalyst, labeled as C_{16}PMo-TiO_2. Supported ionic liquids catalysts with $n = 4$ and 8 were synthesized by a similar method, commercial grade TiO_2, abbreviated as TiO_2 (C), was also used as a carrier to load C_{16}PMo for comparison, and the resulting catalyst was marked as C_{16}PMo-TiO_2 (C).

2.3 Catalyst characterization

Thermogravimetric analysis of samples was conducted on an integrated thermal analyzer STA-449C (TG, NETZSCH Corporation, Germany) from 25 to 800 °C at a heating rate of 10 °C/min in air. Infrared spectroscopy of catalysts was used to detect Keggin structures on a Nicolet Nexus 470 Fourier transform infrared spectrometer (Thermo Fisher Scientific, USA) from wavenumber from 4000 to 400 cm^{-1}. A UV–visible spectrometer UV-2450 (DRS, Shimadzu Corporation, Japan) was used for the diffuse reflectance spectra of 200–800 nm where $BaSO_4$ was used as the diffuse reflective substrate. Wide-angle X-ray diffraction was performed on D/max 2500PC X-ray diffractometer (Rigaku Corporation, Japan) with high-intensity Cu–Ka radiation. To measure the surface area, pore diameter and pore volume of samples, N_2 adsorption and desorption isotherms were collected on a TriStar II 3020 (Micromeritics Instrument Corporation, USA). X-ray photoelectron spectroscopy was carried out using a PHI 5300 XPS (Thermo Electron Corporation, USA). Gas chromatography–mass spectrometry (GC–MS) with an Agilent 7890/5975C (Agilent Corporation, USA) was used for the detection of remaining organic sulfur compounds in the oil phase and further discussion of mechanism in the catalysis reaction.

2.4 Oxidative desulfurization of model oil

The different substrate model oil with 500 ppm sulfur was obtained by, respectively, adding BT, DBT, 3-MBT and 4-MDBT in n-octane as a solvent and denoted as 500 ppm BT, 500 ppm DBT, 500 ppm 3-MBT and 500 ppm 4-MDBT. A proper amount of supported ionic liquid catalyst was mixed with extracting agent ionic liquids blended in 5 mL model oil. The multiphase-dispersed reactive solution was stirred with a magnetic stirrer at 900 rpm for 15 min in a customized 40-mL two-neck flask at the set temperature. Subsequently after 15 min agitation, a proper volume of 30% H_2O_2 was added as the oxidative reagent for the oil phase desulfurized reaction. Afterward, the upper stable layer of the reactor could be aspirated with a microsyringe for analysis of the remaining sulfur content in the model oil. The exact sulfur compound of model oil after the reaction was determined by GC–MS with a flame ionization detector (FID), using n-tetradecane as an internal standard. The chromatographic column parameters were HP-5, 30 m × 0.32 mm i.d. × 0.25 mm. Other parameters are as follows: high-purity nitrogen was the gas carrier; injector temperature of 250 °C; detector temperature of 300 °C.

To calculate the desulfurization rate, the formula used is:

$$\text{Desulfurization rate}(\%) = \left(1 - \frac{\text{Sulfur content after reaction}}{\text{Initial sulfur content}}\right) \times 100.$$

3 Results and discussion

3.1 Composition and structural characterization of C_{16}PMo IL

Figure 1 shows that the thermal decomposition procedure of C_{16}PMo IL underwent three apparent thermodynamic temperature courses. Below 250 °C, C_{16}PMo IL was considered to be in a thermodynamically stable state. The slope of the TG curve declined first between 280 and 400 °C, indicating a collapse of the hexadecane branch in C_{16}PMo IL (Zhang et al. 2013; Xun et al. 2015). The second dramatic fall of the curve appeared from 400 to 600 °C, attributed to anion decomposition in the phosphomolybdic acid-modified ionic liquid. The third period of mass loss appeared from 600 to 800 °C, attributed to the collapse of the imidazole ring. Based on the result of TG

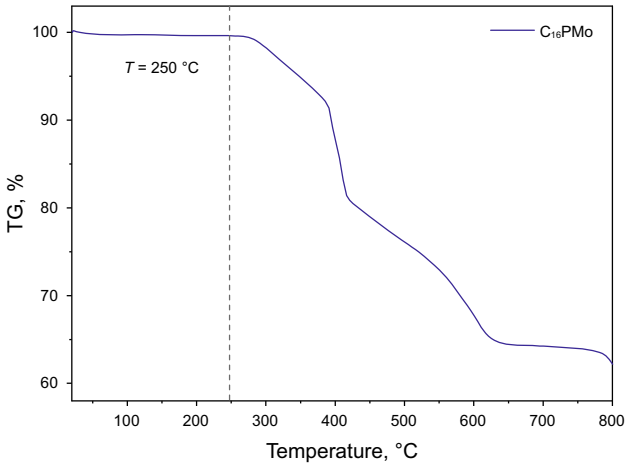

Fig. 1 TG characterization of the $C_{16}PMo$ IL

analysis, an interpretation could be drawn that in the synthesis process of supported ionic liquid catalyst, the structure of the ionic liquid was not damaged by the heat treatment below 250 °C.

The FTIR spectra of $C_{16}PMo$ IL and the supported catalysts with different ILs are shown in Fig. 2. The peaks around 798 cm^{-1}, 879 cm^{-1}, 960 cm^{-1} and 1058 cm^{-1} in Fig. 2a were the Keggin structure characteristic bands of $C_{16}PMo$ IL (Mendez et al. 2013). The bands at 960 cm^{-1} and 1058 cm^{-1} attributed to the Keggin structure in the supported catalysts, and characteristic peaks found at 570-630 cm^{-1} and 1401 cm^{-1} corresponded to Ti–O bonds in TiO_2, which proved the successful loading of ionic liquids on the carrier TiO_2 (Zou et al. 2010). Apart from that, the broad absorption peaks, around 3280–3360 cm^{-1}, corresponded to O–H vibrations for Ti–OH stretching vibration as well as physisorbed water molecules on the surface of catalyst (Yu et al. 2003). Meanwhile, inconspicuous characteristic peaks of the C=N double bond at 1567 cm^{-1}, representing the presence of an imidazole ring, could be observed in the FTIR spectra.

The UV–vis spectra of $C_{16}PMo$ IL and as-prepared supported catalysts are presented in Fig. 3. The high-intensity peaks could be observed in all prepared samples from the wavelength of 200 to 400 nm, corresponding to the characteristic peaks of TiO_2. It could be seen in Fig. 3a that the signal around 230 nm (Zhu et al. 2011) was consistent with the absorption peak of $C_{16}PMo$ ionic liquids, which was apparently detected after loading $C_{16}PMo$ IL on TiO_2 support (Fig. 3d, e). In the region of 200–300 nm, no obvious characteristic peaks of C_4PMo and C_8PMo ILs were found in Fig. 3b, c, indicating the strong absorption peak of TiO_2 support had an influence on the absorption peaks of C_4PMo and C_8PMo ILs.

Wide-angle XRD patterns are used to investigate the change in the crystal morphology of supported ionic liquid catalysts. The single absorption peak of $C_{16}PMo$ ILs at $2\theta = 9.3°$ can be viewed in Fig. 4a. And the samples showed broad peaks at $2\theta = 26.5°$ (Fig. 4b–d), indicating the presence of the amorphous TiO_2 carrier. In addition, no other characteristic absorption peak of TiO_2 was detected. Obviously, the catalyst prepared from purchased commercial grade TiO_2 had XRD peaks, corresponding to the anatase phase of TiO_2. The sharp diffraction peak of the ionic liquid almost completely disappeared in all supported catalysts, which might be the low ionic liquids content and good dispersion.

N_2 adsorption–desorption isotherms and pore size distribution of the catalysts are shown in Fig. 5(a, b). Three kinds of supported C_nPMo (n = 4, 8, 16) IL catalysts with as-prepared TiO_2 exhibited a type II isotherm, which implied the existence of a microporous structure.

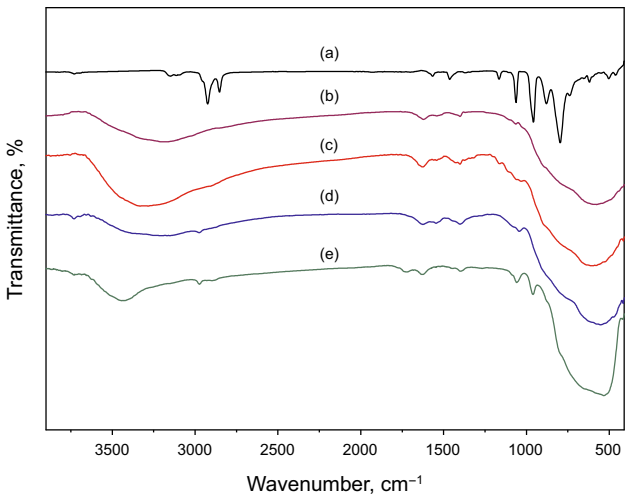

Fig. 2 FTIR spectra of *a* $C_{16}PMo$, *b* C_4PMo-TiO_2, *c* C_8PMo-TiO_2, *d* $C_{16}PMo$-TiO_2, *e* $C_{16}PMo$-TiO_2 (C)

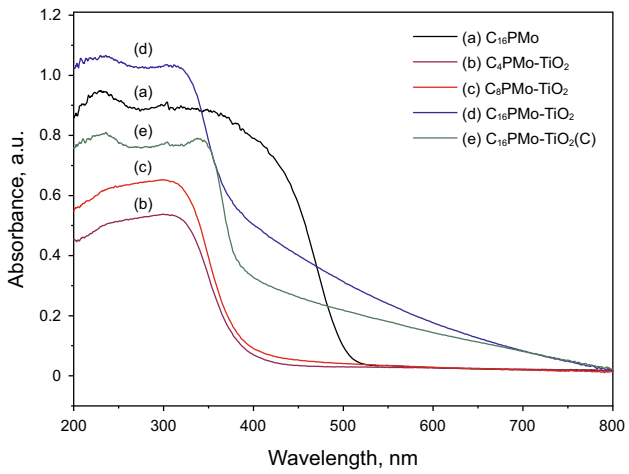

Fig. 3 DRS spectra of *a* $C_{16}PMo$, *b* C_4PMo-TiO_2, *c* C_8PMo-TiO_2, *d* $C_{16}PMo$-TiO_2, *e* $C_{16}PMo$-TiO_2 (C)

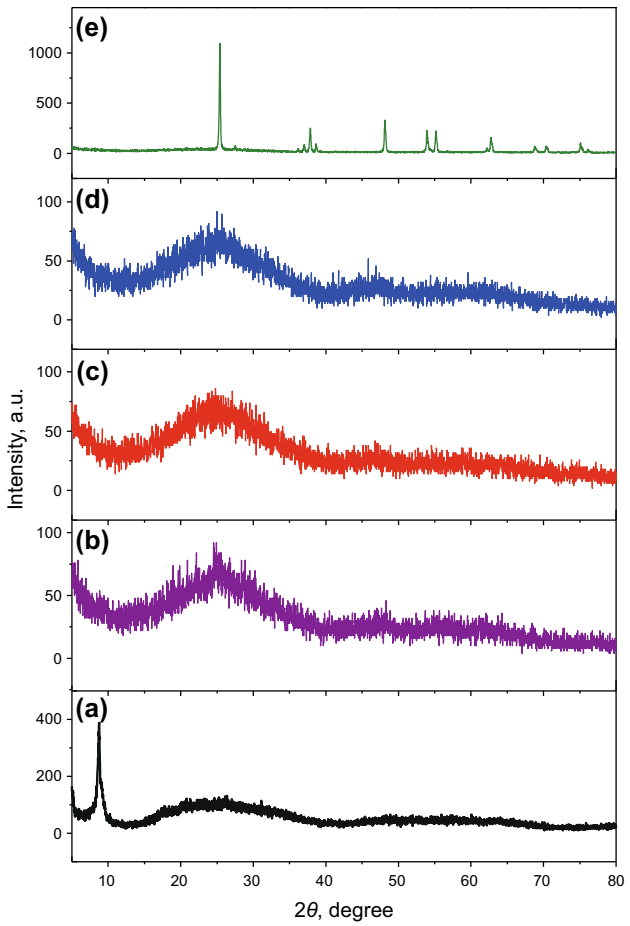

Fig. 4 Wide-angle XRD patterns of **a** C_{16}PMo, **b** C_4PMo-TiO_2, **c** C_8PMo-TiO_2, **d** C_{16}PMo-TiO_2, **e** C_{16}PMo-TiO_2 (C)

Meanwhile, the catalyst produced with commercial grade TiO_2 support represented a type IV isotherm, denoting that a lot of accumulation holes were created (Yan et al. 2013).

As shown in Table 1, the pore diameters of C_4PMo-TiO_2, C_8PMo-TiO_2 and C_{16}PMo-TiO_2 were all observed to be less than 10 nm, and they were slightly smaller than that of C_{16}PMo-TiO_2 (C). In addition, the surface area of commercial TiO_2-supported catalyst remained very small, implying that commercial grade TiO_2 was not a suitable carrier to load C_{16}PMo IL. Moreover, with the growth of the carbon chain length, the specific surface area of C_4PMo-TiO_2, C_8PMo-TiO_2 and C_{16}PMo-TiO_2 increased gradually, but the mean pore diameter and pore volume decreased. Above all, the length of the carbon chain in ionic liquids could influence the morphology of the supported catalysts greatly and would further affect the desulfurization activities.

XPS analysis was performed to investigate the chemical states of the elements in the catalysts. The XPS full spectrum of the catalyst showed that the catalyst consisted of C, N, O, Ti, P and Mo, and binding energy of individual element is shown in Fig. 6a. From Fig. 6b, Mo 3*d* could be divided into two apparent peaks Mo $3d_{3/2}$ and Mo $3d_{5/2}$, respectively, parallel to the electron binding energy of 235.0 eV and 231.9 eV. Ti 2*p* in Fig. 6c was split into two peaks at electron binding energy of 458.2 eV and 463.9 eV, respectively, corresponding to characteristic peaks of Ti $2p_{3/2}$ and Ti $2p_{1/2}$ (Wang et al. 2015). The XPS results indicated that C_{16}PMo ionic liquid was loaded on TiO_2 successfully, which are consistent with the results of FTIR spectra discussed above.

3.2 Effect of different kinds of ILs supported catalysts on the removal of DBT

The DBT removal rates of supported catalysts with different ILs are shown in Table 2 (diesel model oil). When

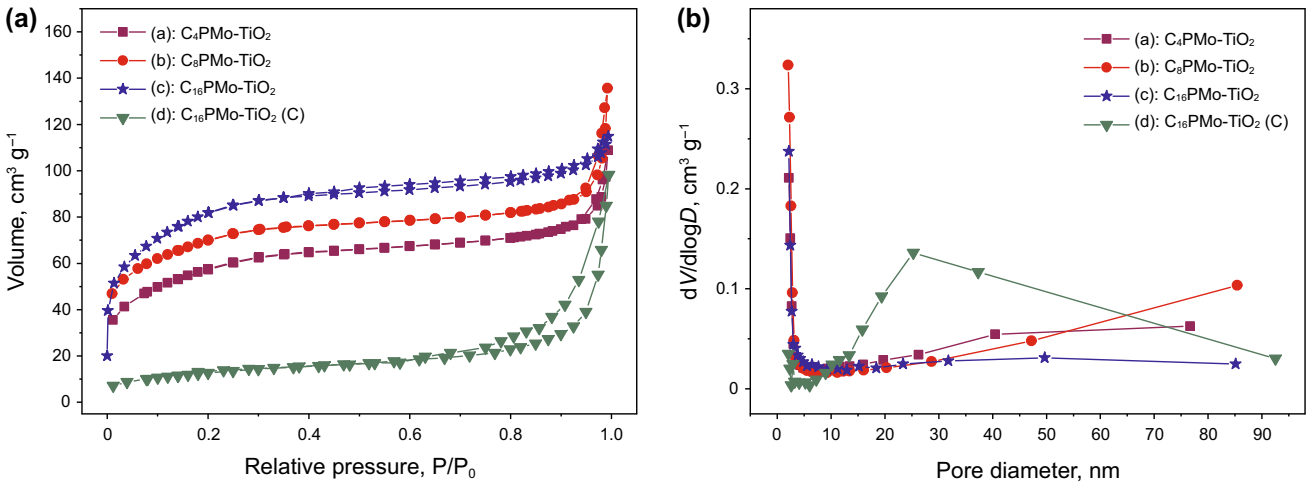

Fig. 5 Nitrogen adsorption–desorption isotherms (**a**) and pore size distributions (**b**) of the catalysts, *a* C_4PMo-TiO_2, *b* C_8PMo-TiO_2, *c* C_{16}PMo-TiO_2, *d* C_{16}PMo-TiO_2 (C)

Table 1 Textural properties of all prepared samples

Samples	Surface area, m^2/g	Pore diameter, nm	Pore volume, cm^3/g
$C_4PMo\text{-}TiO_2$	202.5	7.3	0.100
$C_8PMo\text{-}TiO_2$	251.0	6.3	0.081
$C_{16}PMo\text{-}TiO_2$	284.0	4.6	0.065
$C_{16}PMo\text{-}TiO_2$ (C)	4.6	17.7	0.010

0.01 g of $C_4PMo\text{-}TiO_2$ or $C_8PMo\text{-}TiO_2$ was applied, 80.1% and 82.6% desulfurization rates could be obtained, respectively. Under the same experimental conditions, 85.8% of DBT was eliminated by $C_{16}PMo\text{-}TiO_2$ after 30 min, showing the highest efficiency of the three catalysts. The good catalytic activity of $C_{16}PMo\text{-}TiO_2$ attributed to more hydrophobicity of long carbon chains than short ones, like $C_4PMo\text{-}TiO_2$ and $C_8PMo\text{-}TiO_2$, which made the supported catalyst contact with oil phase more easily. Therefore, $C_{16}PMo\text{-}TiO_2$ was chosen to employ in further experiments to investigate the effect of different reaction systems.

3.3 Effect of different desulfurization systems on the removal of DBT

Different desulfurization conditions for removal of DBT were examined with $C_{16}PMo\text{-}TiO_2$ (Table 3). When no extractant was added, the catalyst was more likely to stick to the bottom of the flask, and the removal of DBT was only 7.8%. Without the catalyst, the desulfurization rate was 17.1% by only adding extractant, forming the simple extractive coupled oxidative desulfurization system. When catalyst and extractant were simultaneously added in the reaction flask, an extractive coupled catalytic oxidative desulfurization system was formed. Under the same conditions, DBT was totally removed, indicating the achievement of deep desulfurization. The performance of $C_{16}PMo$ IL loaded on commercial grade TiO_2 catalyst was also been investigated. In ECODS system, the desulfurization rate was only 18% after 1 h. Compared to commercial grade TiO_2, amorphous TiO_2 was a more suitable support to load ILs. In summary, the experiment indicated both ILs and support importantly affect the results of oxidative desulfurization.

3.4 Effect of amount of catalysts on the removal of DBT

In the process of oxidative desulfurization, the mass of catalyst was important to sulfur removal. As shown in Fig. 7, the desulfurization rates increased by increasing the amount of catalyst at equal time intervals. Generally, the sulfur removal rate was obviously increased when the reaction time was extended. After 1 h reaction, a 96.0% desulfurization rate was attained by adding 5 mg catalyst in model oil. When the mass of catalyst was increased to 10 mg, 100% removal of DBT was achieved after 1 h reaction and 100% DBT was removed in 50 min when 15 mg catalyst was added. For material saving, 10 mg catalyst was chosen to be used in the ECODS system.

3.5 Effect of reaction temperature on the removal of DBT

In order to study the influence of reaction temperature on the desulfurization, temperatures between 30 and 60 °C were selected in the experiments and the results are shown in Fig. 8. The desulfurization rate increased when the reaction temperature was raised. At 30 °C, the desulfurization rate of the system increased slowly, only to 53.7% in 1.5 h. It indicated that at low temperature, the catalytic activity of the supported ionic liquid was poor. When the reaction temperature was raised to 40 °C, 97.3% desulfurization rate was achieved after 1.5 h. When the temperature was raised to 50 °C, a complete removal of DBT was attained for 1 h reaction. Significantly, with the progress of the reaction, the desulfurization rate increased rapidly. As the reaction temperature was raised up to 60 °C, 100% DBT could be removed in only 40 min. For the efficient desulfurization and energy saving, 50 °C was the most suitable reaction temperature in this system.

3.6 Effect of different extractants on the removal of DBT

The desulfurization rate is deeply affected by extractants with different properties, so four types of conventional ionic liquids were selected as extractants to test the influence on the removal of DBT. Results are shown in Table 4, desulfurization systems with different extractants were taken for initial 15 min extraction to attain the extraction balance (Li et al. 2012), and then the property of extraction of each ionic liquid was obtained. The order of extracting activities of four types of conventional ionic liquids was $[Omim]BF_4$ (31.1%) > $[Omim]PF_6$ (21.8%) > $[Bmim]BF_4$ (18.6%) > $[Bmim]PF_6$ (15.1%). The result implied that the performance of long-chain ILs was better than the short-chain ILs in terms of extractive desulfurization. In the ECODS systems, a certain amount of H_2O_2

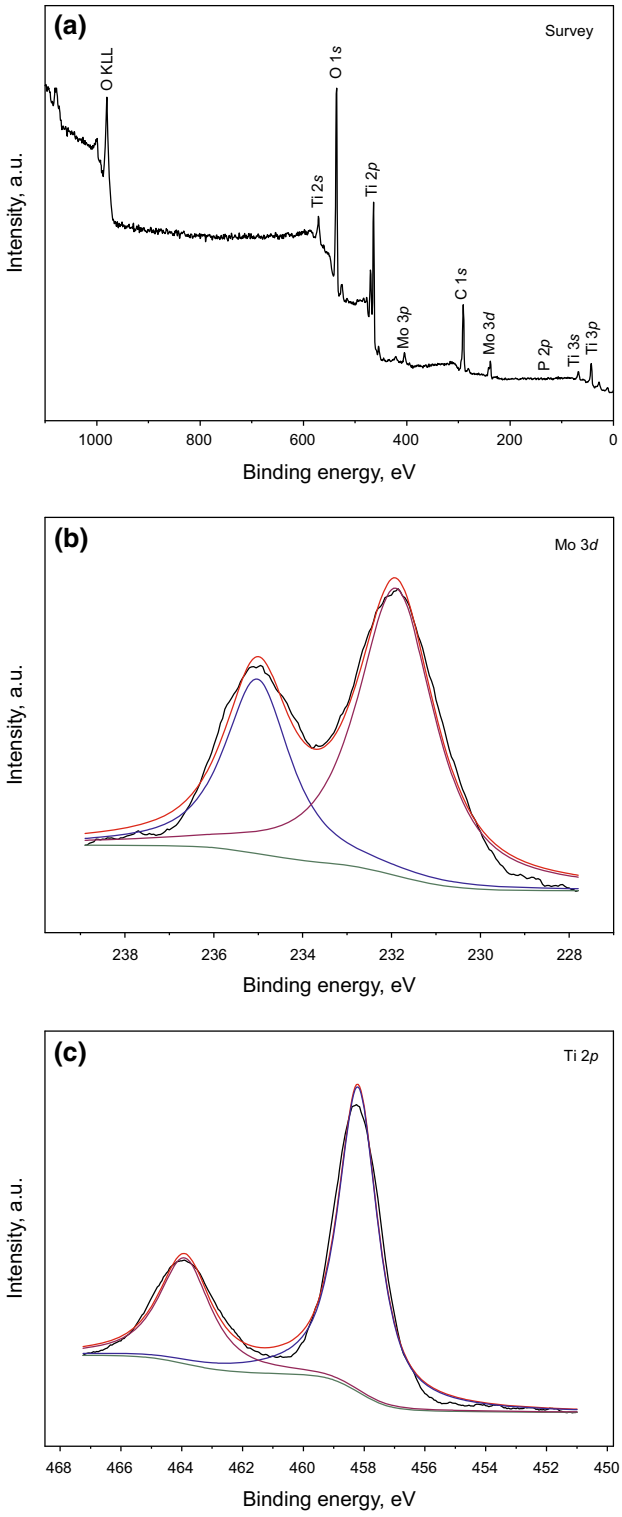

Fig. 6 XPS spectra of $C_{16}PMo\text{-}TiO_2$. **a** Survey of the catalyst, **b** Mo 3*d* and **c** Ti 2*p*

(n(O)/n(S) molar ratio was 3) was added and reacted for 1 h, and the sulfur removal rates were 99.9%, 57.2%, 100% and 24.0%, respectively. Above all, $[Bmim]BF_4$ was the most suitable extractant considering efficiency and economics.

Table 2 Effect of the length of carbon chains on the removal of DBT

Entry	Different catalysts	Sulfur removal, %
1	$C_4PMo\text{-}TiO_2$	80.1
2	$C_8PMo\text{-}TiO_2$	82.6
3	$C_{16}PMo\text{-}TiO_2$	85.8

Experimental conditions: m (catalyst) = 0.01 g, $V([Bmim]BF_4)$ = 1 mL, T = 50 °C, molar ratio n(O)/n(S) = 3, t = 30 min, V(model oil) = 5 mL

Table 3 Effect of different desulfurization systems on removal of DBT

Entry	Different catalysts	Extractant	Sulfur removal, %
1	$C_{16}PMo\text{-}TiO_2$	–	7.8
2	–	+	17.1
3	$C_{16}PMo\text{-}TiO_2$	+	100
4	$C_{16}PMo\text{-}TiO_2$ (C)	+	18.0

Experimental conditions: m (catalyst) = 0.01 g, $V([Bmim]BF_4)$ = 1 mL, T = 50 °C, molar ratio n(O)/n(S) = 3, t = 1 h, V(model oil) = 5 mL

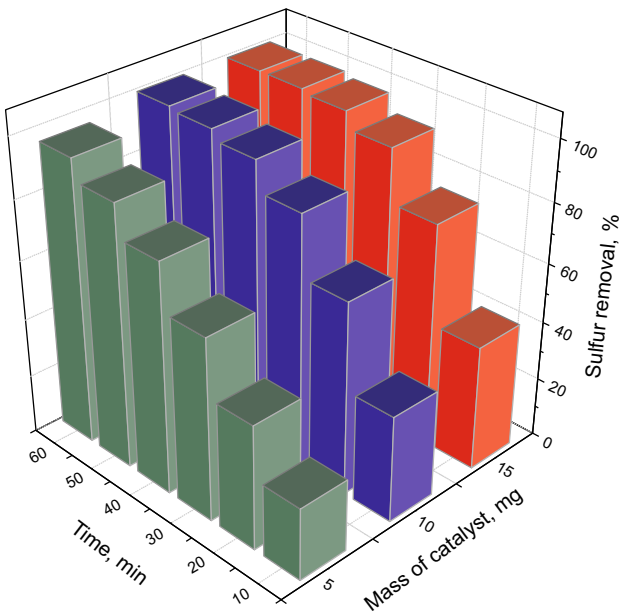

Fig. 7 Effect of the amount of catalyst on the removal of DBT. Experimental conditions: $V([Bmim]BF_4)$ = 1 mL, T = 50 °C, t = 1 h, molar ratio n(O)/n(S) = 3, V(model oil) = 5 mL

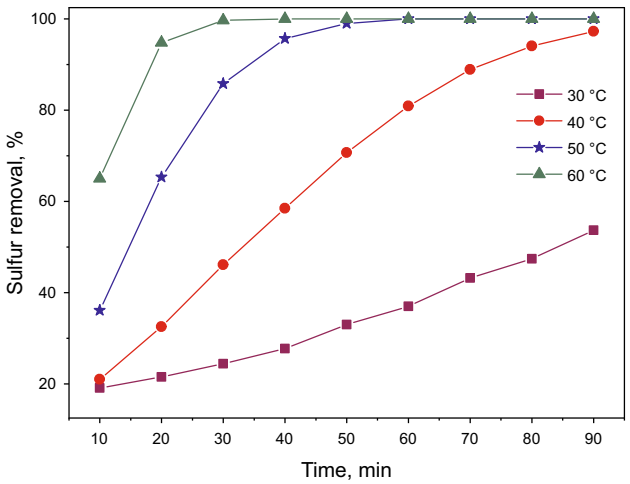

Fig. 8 Effect of reaction temperatures on the removal of DBT. Experimental conditions: m (catalyst) = 0.01 g, V([Bmim]BF_4)- = 1 mL, molar ratio n(O)/n(S) = 3, V(model oil) = 5 mL

Table 4 Effect of different types of extractants on removal of DBT

Entry	Different ILs	Sulfur removal, %	
		EDS[a]	ECODS[b]
1	[Bmim]PF_6	15.1	24.0
2	[Omim]PF_6	21.8	57.2
3	[Bmim]BF_4	18.6	100
4	[Omim]BF_4	31.1	99.9

Experiment conditions: m (catalyst) = 0.01 g, V(IL) = 1 mL, molar ratio n(O)/n(S) = 3, T = 50 °C, V(model oil) = 5 mL

[a] t = 15 min

[b] t = 1 h

3.7 Effect of different n(O)/n(S) molar ratios on the removal of DBT

In ECODS system, the removal of DBT was also affected by the amount of oxidant. According to the stoichiometric ratio, 2 mol of hydrogen peroxide is needed to oxidize 1 mol of sulfide to its corresponding sulfone. The effect of the amount of hydrogen peroxide on the desulfurization rate is shown in Fig. 9. When an n(O)/n(S) molar ratio of 2:1 was applied, the removal rate of DBT increased rapidly first and then tended to be steady, and after 1 h reaction, the desulfurization rate was 92.1%. When the n(O)/n(S) molar ratio of hydrogen peroxide increased to 3:1, the corresponding desulfurization rate reached 100%. When n(O)/n(S) molar ratio increased to 4:1, the DBT was completely removed in only 50 min. Taken together, 3:1 molar ratio of n(O)/n(S) and 1 h reaction were the more appropriate reaction conditions in the ECODS system.

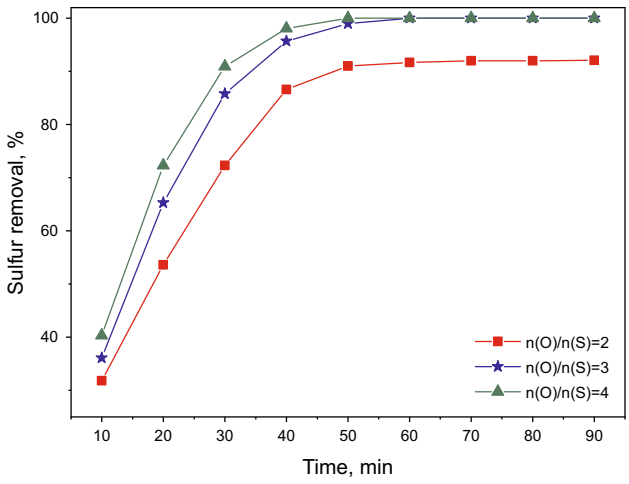

Fig. 9 Effect of n(O)/n(S) molar ratios on the removal of DBT. Experimental conditions: m (catalyst) = 0.01 g, V([Bmim]BF_4)- = 1 mL, T = 50 °C, V(model oil) = 5 mL

3.8 Effect of different substrates in the ECODS system

BT, 3-MBT and 4-MDBT, which function as the aromatic reaction substrates, were selected to investigate the desulfurization activities in the ECODS system. As shown in Fig. 10, the ECODS system had different removal rates on various reaction substrates. After 1.5 h reaction, the removal rates of the three substrates BT, 3-MBT and 4-MDBT were 63.5%, 97.7% and 49.4%, respectively. Significantly, the differences were mainly due to two factors, namely the electron cloud density of the sulfur element on different sulfur compounds and the steric hindrance effect caused by methyl groups. Based on the

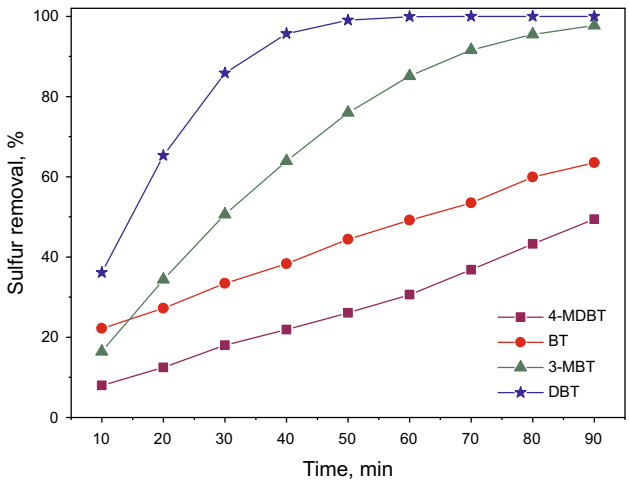

Fig. 10 Catalytic performance of different sulfur-containing substrates. Experimental conditions: m (catalyst) = 0.01 g, V([Bmim]BF_4) = 1 mL, T = 50 °C, molar ratio n(O)/n(S) = 3, V(-model oil) = 5 mL

calculation by Otsuki et al. (2000), the electron cloud density of the sulfur atoms on DBT and 4-MDBT was 5.758 and 5.759, respectively. However, the removal rate of 4-MDBT was apparently lower than that of DBT; it might be attributed to steric hindrance originated by the methyl group on the 4-MDBT that hinders the removal reaction. For DBT and BT, these two model sulfides were all constructed without the methyl group; therefore, steric hindrance could not affect the desulfurization rates. The desulfurization process was mainly influenced by the electron density of the sulfur atoms, the electronic cloud density of the sulfur atom on BT (5.568) was lower than that on DBT, and the actual desulfurization rate of BT was less than that of DBT. Notably, the methyl group on 3-MBT was away from the sulfur atom, so without the effect of steric hindrance, the contract reaction between the active center and sulfur element could undergo a normal activation of the oxidation process. Meanwhile, the increase of electronic cloud density on sulfur (5.572) (Li et al. 2015) was due to the electron donating effect of the methyl group, which made 3-MBT more easily to be removed in the oxidative process. Above all, the oxidative efficiencies of the four substrates decreased in the following order: DBT > 3-MBT > BT > 4-MDBT.

3.9 Analysis of the oxidation products and proposed mechanism

After the oxidative process, model oil was enriched in the upper part of the reactor and the products could be analyzed directly by GC–MS. As shown in Fig. 11a, the desulfurization rate was 100% and neither DBT residual signal nor signals of other sulfur compounds were found in the oil phase. After that, the lower ionic liquids phase was extracted with carbon tetrachloride and further analyzed by GC–MS. The results are shown in Fig. 11b; a small amount of residual DBT (m/z = 184.0) and $DBTO_2$ (m/z = 216.0) could be detected (Xun et al. 2016). Because of the extraction effect of ionic liquids, a small amount of DBT was found without further oxidation into $DBTO_2$. Apart from that, no other forms of sulfur compounds were found in the IL phase, indicating that $DBTO_2$ was the only product in the oxidative desulfurization. According to the above results, a possible ECODS mechanism was proposed and presented in Scheme 1. With the action of hydrogen peroxide, Mo=O double bonds in polyoxometalate ionic liquid was converted to peroxo-molybdenum species first [abbreviated as $Mo(O_2)$] (Garcia-Gutierrez et al. 2008; Zhang et al. 2014a) and then combined with DBT, and DBT was oxidized into the corresponding sulfone ($DBTO_2$). After the reaction, the oxidative products were preserved in the ionic liquid phase and clean oil was eventually obtained.

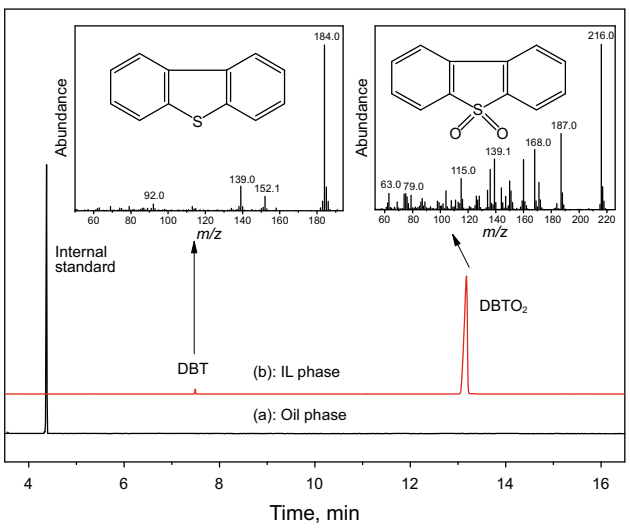

Fig. 11 GC–MS analysis of main compounds in the oil phase (**a**) and ionic liquid phase (**b**) after the reaction

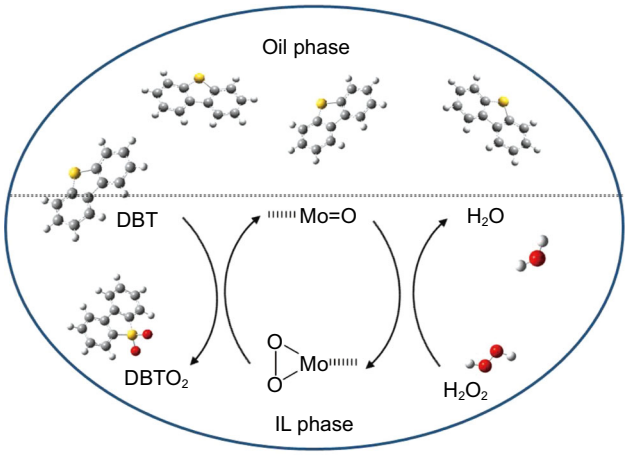

Scheme 1 Possible mechanism of the ECODS system

3.10 Cyclic performance of the supported IL catalyst

The supported catalyst $C_{16}PMo\text{-}TiO_2$ could be recovered easily by filtration, and the results of recyclability are shown in Fig. 12. The removal of DBT only decreased 3.1% to 96.9% from 100% when eight cycle experiments were conducted. The continuation of the cycle experiments found that the desulfurization rates were 94.6% and 92.9% in the ninth and tenth cycles, respectively. The drop could be ascribed to the enrichment of $DBTO_2$ in the IL phase and $DBTO_2$ covering the surface of the catalyst, which partially hindered the activity center contact with the model oil. Notably, the catalysts presented outstanding sulfur removal rates with no apparent decrease after eight

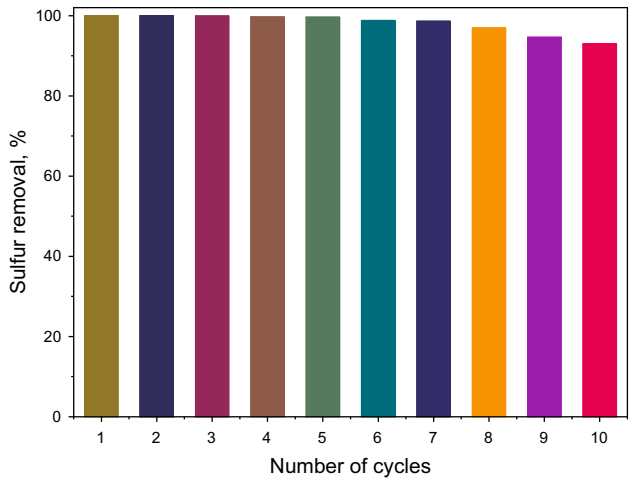

Fig. 12 Recycle performance of the $C_{16}PMo\text{-}TiO_2$ catalyst. Experimental conditions: m (catalyst) = 0.01 g, V([Bmim]BF_4) = 1 mL, T = 50 °C, molar ratio n(O)/n(S) = 3, t = 1 h, V(model oil) = 5 mL

cycles, indicating the great recyclability and the potential industrial application.

4 Conclusion

Firstly, novel types of supported IL catalysts $[C_n mim]_3PMo_{12}O_{40}/Am\ TiO_2$ (n = 4, 8, 16) were prepared through a one-step method. Characterizations such as FTIR, DRS, wide-angle XRD, N_2 adsorption–desorption, XPS and other analytical techniques were applied to analyze the structure and composition of synthetic catalysts. The results revealed the successful preparation, and the structure of the ionic liquids was preserved. Secondly, the catalytic activities of the designed catalysts were investigated in ECODS systems, and various factors that affect the desulfurization rates were studied. DBT in the model oil could be removed completely under optimal conditions, meeting the aim of deep desulfurization. Thirdly, the desulfurization effects on various substrates were studied, and the activity order in this catalytic system was: DBT > 3-MBT > BT > 4-MDBT. Importantly, the experiments showed that after ten cycles, the desulfurization activity of $[C_{16}mim]_3PMo_{12}O_{40}/Am\ TiO_2$ only dropped from 100% to 92.9%, indicating the good recycling performance of the catalyst and the potential industrial application.

Acknowledgements This work was financially supported by the National Natural Science Foundation of China (Nos. 21576122, 21646001, 21506080), Natural Science Foundation of Jiangsu Province (Nos. BK20150485, BK20170528), China Postdoctoral Science Foundation (2017M611727) and Jiangsu Planned Projects for Postdoctoral Research Funds (1701104B), and supported by the Student Innovation and Entrepreneurship Training Program (201810299332 W).

References

Ahmed I, Panja T, Khan NA, Sarker M, Yu J-S, Jhung SH. Nitrogen-doped porous carbons from ionic liquids@MOF: remarkable adsorbents for both aqueous and nonaqueous media. ACS Appl Mater Inter. 2017;9(11):10276–85. https://doi.org/10.1021/acsami.7b00859.

Alejandro Dinamarca M, Rojas A, Baeza P, Espinoza G, Ibacache Quiroga C, Ojeda J. Optimizing the biodesulfurization of gas oil by adding surfactants to immobilized cell systems. Fuel. 2014;116:237–41. https://doi.org/10.1016/j.fuel.2013.07.108.

Alsalme A, Alzaqri N, Alsaleh A, Siddiqui MRH, Alotaibi A, Kozhevnikova EF, et al. Efficient Ni-Mo hydrodesulfurization catalyst prepared through Keggin polyoxometalate. Appl Catal B Environ. 2016;182:102–8. https://doi.org/10.1016/j.apcatb.2015.09.018.

Bhadra BN, Song JY, Khan NA, Jhung SH. TiO_2-containing carbon derived from a metal-organic framework composite: a highly active catalyst for oxidative desulfurization. Acs Appl Mater Inter. 2017;9(36):31192–202. https://doi.org/10.1021/acsami.7b10336.

Chica A, Corma A, Domine ME. Catalytic oxidative desulfurization (ODS) of diesel fuel on a continuous fixed-bed reactor. J Catal. 2006;242(2):299–308. https://doi.org/10.1016/j.jcat.2006.06.013.

Dai C, Zhang J, Huang C, Lei Z. Ionic liquids in selective oxidation: catalysts and solvents. Chem Rev. 2017;117(10):6929–83. https://doi.org/10.1021/acs.chemrev.7b00030.

Domanska U, Wlazlo M. Effect of the cation and anion of the ionic liquid on desulfurization of model fuels. Fuel. 2014;134:114–25. https://doi.org/10.1016/j.fuel.2014.05.048.

Elwan HA, Zaky MT, Farag AS, Soliman FS, Ezel DHM. A coupled extractive-oxidative process for desulfurization of gasoline and diesel fuels using a bifunctional ionic liquid. J Mol Liq. 2017;248:549–55. https://doi.org/10.1016/j.molliq.2017.10.077.

Gao PF, Liu YX, Zhang LN, Zhang SM, Li HW, Wu YQ, et al. Cell receptor screening for human papillomavirus invasion by using a polyoxometalate-peptide assembly as a probe. J Colloid Interface Sci. 2018;514:407–14. https://doi.org/10.1016/j.jcis.2017.12.055.

Garcia-Gutierrez JL, Fuentes GA, Hernandez-Teran ME, Garcia P, Murrieta-Guevara F, Jimenez-Cruz F. Ultra-deep oxidative desulfurization of diesel fuel by the $Mo/Al_2O_3\text{-}H_2O_2$ system: the effect of system parameters on catalytic activity. Appl Catal A Gen. 2008;334(1–2):366–73. https://doi.org/10.1016/j.apcata.2007.10.024.

Guldhe A, Singh P, Ansari FA, Singh B, Bux F. Biodiesel synthesis from microalgal lipids using tungstated zirconia as a heterogeneous acid catalyst and its comparison with homogeneous acid and enzyme catalysts. Fuel. 2017;187:180–8. https://doi.org/10.1016/j.fuel.2016.09.053.

Ibrahim MH, Hayyan M, Hashim MA, Hayyan A. The role of ionic liquids in desulfurization of fuels: a review. Renew Sustain Energy Rev. 2017;76:1534–49. https://doi.org/10.1016/j.rser.2016.11.194.

Jiang B, Yang HW, Zhang LH, Zhang RY, Sun YL, Huang Y. Efficient oxidative desulfurization of diesel fuel using amide-based ionic liquids. Chem Eng J. 2016;283:89–96. https://doi.org/10.1016/j.cej.2015.07.070.

Jiang W, Zheng D, Xun SH, Qin YJ, Lu QQ, Zhu WS, et al. Polyoxometalate-based ionic liquid supported on graphite carbon induced solvent-free ultra-deep oxidative desulfurization of model fuels. Fuel. 2017;190:1–9. https://doi.org/10.1016/j.fuel.2016.11.024.

Jiang W, Zhu WS, Chang YH, Chao YH, Yin S, Liu H, et al. Ionic liquid extraction and catalytic oxidative desulfurization of fuels using dialkylpiperidinium tetrachloroferrates catalysts. Chem Eng J. 2014;250:48–54. https://doi.org/10.1016/j.cej.2014.03.074.

Khan NA, Jhung SH. Adsorptive removal and separation of chemicals with metal-organic frameworks: contribution of pi-complexation. J Hazard Mater. 2017;325:198–213. https://doi.org/10.1016/j.jhazmat.2016.11.070.

Khan NA, Bhadra BN, Jhung SH. Heteropoly acid-loaded ionic liquid@metal-organic frameworks: effective and reusable adsorbents for the desulfurization of a liquid model fuel. Chem Eng J. 2018;334:2215–21. https://doi.org/10.1016/j.cej.2017.11.159.

Khodayari R, Odenbrand CUI. Regeneration of commercial SCR catalysts by washing and sulphation: effect of sulphate groups on the activity. Appl Catal B Environ. 2001;33(4):277–91. https://doi.org/10.1016/s0926-3373(01)00193-x.

Kim M-S, Chung S-H, Yoo C-J, Lee MS, Cho I-H, Lee D-W, et al. Catalytic reduction of nitrate in water over Pd–Cu/TiO_2 catalyst: effect of the strong metal-support interaction (SMSI) on the catalytic activity. Appl Catal B Environ. 2013;142–143:354–61. https://doi.org/10.1016/j.apcatb.2013.05.033.

Li HM, Zhu WS, Wang Y, Zhang JT, Lu JD, Yan YS. Deep oxidative desulfurization of fuels in redox ionic liquids based on iron chloride. Green Chem. 2009;11(6):810–5. https://doi.org/10.1039/b901127g.

Li FT, Kou CG, Sun ZM, Hao YJ, Liu RH, Zhao DS. Deep extractive and oxidative desulfurization of dibenzothiophene with $C_5H_9NO{\cdot}SnCl_2$ coordinated ionic liquid. J Hazard Mater. 2012;205–206:164–70. https://doi.org/10.1016/j.jhazmat.2011.12.054.

Li HP, Zhu WS, Chang YH, Jiang W, Zhang M, Yin S, et al. Theoretical investigation of the interaction between aromatic sulfur compounds and $[BMIM]^+[FeCl_4]^-$ ionic liquid in desulfurization: a novel charge transfer mechanism. J Mol Graph Model. 2015;59:40–9. https://doi.org/10.1016/j.jmgm.2015.03.007.

Li HP, Zhu WS, Zhu SW, Xia JX, Chang YH, Jiang W, et al. The selectivity for sulfur removal from oils: an insight from conceptual density functional theory. AIChE J. 2016;62(6):2087–100. https://doi.org/10.1002/aic.15161.

Liu YQ, Wang HY, Liu YQ, Zhao JC, Liu CG. Reactive adsorption desulfurization on Cu/ZnO adsorbent: effect of ZnO polarity ratio on selective hydrogenation. Energy Fuel. 2017;31(9):9930–8. https://doi.org/10.1021/acs.energyfuels.7601935.

Mendez FJ, Llanos A, Echeverria M, Jauregui R, Villasana Y, Diaz Y, et al. Mesoporous catalysts based on Keggin-type heteropoly-acids supported on MCM-41 and their application in thiophene hydrodesulfurization. Fuel. 2013;110:249–58. https://doi.org/10.1016/j.fuel.2012.11.021.

Moghadam FR, Azizian S, Bayat M, Yarie M, Kianpour E, Zolfigol MA. Extractive desulfurization of liquid fuel by using a green, neutral and task specific phosphonium ionic liquid with glyceryl moiety: a joint experimental and computational study. Fuel. 2017;208:214–22. https://doi.org/10.1016/j.fuel.2017.07.025.

Morales-Ortuño JC, Klimova TE. Development of new hydrodesulfurization NiMo catalysts supported on Al_2O_3-TiSBA-15 hybrid materials. Fuel. 2017;198:99–109. https://doi.org/10.1016/j.fuel.2017.01.007.

Morales-Ortuño JC, Ortega-Domínguez RA, Hernández-Hipólito P, Bokhimi X, Klimova TE. HDS performance of NiMo catalysts supported on nanostructured materials containing titania. Catal Today. 2016;271:127–39. https://doi.org/10.1016/j.cattod.2015.07.028.

Nan HK, Lee JS, Huh ES, Lee H, Jung KD, Kim HS, et al. Extractive desulfurization using Fe-containing ionic liquids. Energy Fuel. 2008;22(3):1687–90.

Nejad NF, Beigi AAM. Efficient desulfurization of gasoline fuel using ionic liquid extraction as a complementary process to adsorptive desulfurization. Pet Sci. 2015;12(2):330–9. https://doi.org/10.1007/s12182-015-0020-2.

Otsuki S, Nonaka T, Takashima N, Qian WH, Ishihara A, Imai T, et al. Oxidative desulfurization of light gas oil and vacuum gas oil by oxidation and solvent extraction. Energy Fuel. 2000;14(6):1232–9. https://doi.org/10.1021/ef000096i.

Pham XN, Tran DL, Pham TD, Nguyen QM, Thi VTT, Van HD. One-step synthesis, characterization and oxidative desulfurization of 12-tungstophosphoric heteropolyanions immobilized on amino functionalized SBA-15. Adv Powder Technol. 2018;29(1):58–65. https://doi.org/10.1016/j.apt.2017.10.011.

Piccinino D, Abdalghani I, Botta G, Crucianelli M, Passacantando M, Di Vacri ML, et al. Preparation of wrapped carbon nanotubes poly(4-vinylpyridine)/MTO based heterogeneous catalysts for the oxidative desulfurization (ODS) of model and synthetic diesel fuel. Appl Catal B Environ. 2017;200:392–401. https://doi.org/10.1016/j.apcatb.2016.07.037.

Rafiee E, Sahraei S, Moradi GR. Extractive oxidative desulfurization of model oil/crude oil using KSF montmorillonite-supported 12-tungstophosphoric acid. Pet Sci. 2016;13(4):760–9. https://doi.org/10.1007/s12182-016-0127-0.

Rodríguez-Cabo B, Rodríguez H, Rodil E, Arce A, Soto A. Extractive and oxidative-extractive desulfurization of fuels with ionic liquids. Fuel. 2014;117:882–9. https://doi.org/10.1016/j.fuel.2013.10.012.

Selvavathi V, Chidambaram V, Meenalkshisundaram A, Sairam B, Sivasankar B. Adsorptive desulfurization of diesel on activated carbon and nickel supported systems. Catal Today. 2009;141(1–2):99–102. https://doi.org/10.1016/j.cattod.2008.05.009.

Song Z, Zhou T, Qi Z, Sundmacher K. Systematic method for screening ionic liquids as extraction solvents exemplified by an extractive desulfurization process. ACS Sustain Chem Eng. 2017;5(4):3382–9. https://doi.org/10.1021/acssuschemeng.7b00024.

Srivastav A, Srivastava VC. Adsorptive desulfurization by activated alumina. J Hazard Mater. 2009;170(2–3):1133–40. https://doi.org/10.1016/j.jhazmat.2009.05.088.

Vozka P, Orazgaliyeva D, Šimáček P, Blažek J, Kilaz G. Activity comparison of Ni-Mo/Al_2O_3 and Ni-Mo/TiO_2 catalysts in hydroprocessing of middle petroleum distillates and their blend with rapeseed oil. Fuel Process Technol. 2017;167:684–94. https://doi.org/10.1016/j.fuproc.2017.08.019.

Wang DH, Qian EWH, Amano H, Okata K, Ishihara A, Kabe T. Oxidative desulfurization of fuel oil—part I. Oxidation of dibenzothiophenes using tert-butyl hydroperoxide. Appl Catal A Gen. 2003;253(1):91–9. https://doi.org/10.1016/s0926-860x(03)00528-3.

Wang XJ, Yang WY, Li FT, Zhao J, Liu RH, Liu SJ, et al. Construction of amorphous TiO_2/BiOBr heterojunctions via facets coupling for enhanced photocatalytic activity. J Hazard

Mater. 2015;292:126–36. https://doi.org/10.1016/j.jhazmat.2015.03.030.

Xun SH, Zhu WS, Zhu FX, Chang YH, Zheng D, Qin YJ, et al. Design and synthesis of W-containing mesoporous material with excellent catalytic activity for the oxidation of 4,6-DMDBT in fuels. Chem Eng J. 2015;280:256–64. https://doi.org/10.1016/j.cej.2015.05.092.

Xun SH, Zhu WS, Chang YH, Li HP, Zhang M, Jiang W, et al. Synthesis of supported $SiW_{12}O_{40}$-based ionic liquid catalyst induced solvent-free oxidative deep-desulfurization of fuels. Chem Eng J. 2016;288:608–17. https://doi.org/10.1016/j.cej.2015.12.005.

Yan XM, Mei P, Xiong L, Gao L, Yang QF, Gong LJ. Mesoporous titania-silica-polyoxometalate nanocomposite materials for catalytic oxidation desulfurization of fuel oil. Catal Sci Technol. 2013;3(8):1985–92. https://doi.org/10.1039/c3cy20732c.

Yang HW, Jiang B, Sun YL, Zhang LH, Sun ZN, Wang JY, et al. Polymeric cation and isopolyanion ionic self-assembly: novel thin-layer mesoporous catalyst for oxidative desulfurization. Chem Eng J. 2017;317:32–41. https://doi.org/10.1016/j.cej.2017.01.135.

Yao L, Zhang L, Wang R, Chou S, Dong Z. A new integrated approach for dye removal from wastewater by polyoxometalates functionalized membranes. J Hazard Mater. 2016;301:462–70. https://doi.org/10.1016/j.jhazmat.2015.09.027.

Yu JG, Yu HG, Cheng B, Zhao XJ, Yu JC, Ho WK. The effect of calcination temperature on the surface microstructure and photocatalytic activity of TiO_2 thin films prepared by liquid phase deposition. J Phys Chem B. 2003;107(50):13871–9. https://doi.org/10.1021/jp036158y.

Zeng XY, Xiao XY, Li Y, Chen JY, Wang HL. Deep desulfurization of liquid fuels with molecular oxygen through graphene photocatalytic oxidation. Appl Catal B Environ. 2017;209:98–109. https://doi.org/10.1016/j.apcatb.2017.02.077.

Zhang H, Zhang Q, Zhang L, Pei T, Dong L, Zhou P, et al. Acidic polymeric ionic liquids based reduced graphene oxide: an efficient and rewriteable catalyst for oxidative desulfurization. Chem Eng J. 2018;334:285–95. https://doi.org/10.1016/j.cej.2017.10.042.

Zhang J, Wang AJ, Wang YJ, Wang HY, Gui JZ. Heterogeneous oxidative desulfurization of diesel oil by hydrogen peroxide: catalysis of an amphipathic hybrid material supported on SiO_2. Chem Eng J. 2014a;245:65–70. https://doi.org/10.1016/j.cej.2014.01.103.

Zhang LH, Wang JY, Sun YL, Jiang B, Yang HW. Deep oxidative desulfurization of fuels by superbase-derived Lewis acidic ionic liquids. Chem Eng J. 2017a;328:445–53. https://doi.org/10.1016/j.cej.2017.07.060.

Zhang M, Wei YC, Li R, Zhu WS, Li HP, Zhang Q, et al. Magnetic POM-based mesoporous silica for fast oxidation of aromatic sulfur compounds. Fuel. 2017b;209:545–51. https://doi.org/10.1016/j.fuel.2017.08.001.

Zhang M, Zhu WS, Li HM, Xun SH, Ding WJ, Liu JJ, et al. One-pot synthesis, characterization and desulfurization of functional mesoporous W-MCM-41 from POM-based ionic liquids. Chem Eng J. 2014b;243:386–93. https://doi.org/10.1016/j.cej.2013.12.093.

Zhang M, Zhu WS, Xun SH, Li HM, Gu QQ, Zhao Z, et al. Deep oxidative desulfurization of dibenzothiophene with POM-based hybrid materials in ionic liquids. Chem Eng J. 2013;220:328–36. https://doi.org/10.1016/j.cej.2012.11.138.

Zhang Y, Lin B, Sun Y, Han P, Wang J, Ding X, et al. MoO_2@Cu@C composites prepared by using polyoxometalates@metal-organic frameworks as template for all-solid-state flexible supercapacitor. Electrochim Acta. 2016;188:490–8. https://doi.org/10.1016/j.electacta.2015.12.037.

Zheng B, Wang J, Wang FB, Xia XH. Synthesis of nitrogen doped graphene with high electrocatalytic activity toward oxygen reduction reaction. Electrochem Commun. 2013;28:24–6. https://doi.org/10.1016/j.elecom.2012.11.037.

Zhu WS, Huang WL, Li HM, Zhang M, Jiang W, Chen GY, et al. Polyoxometalate-based ionic liquids as catalysts for deep desulfurization of fuels. Fuel Process Technol. 2011;92(10):1842–8. https://doi.org/10.1016/j.fuproc.2011.04.030.

Zou JA, Gao JC, Xie FY. An amorphous TiO_2 sol sensitized with H_2O_2 with the enhancement of photocatalytic activity. J Alloys Compd. 2010;497(1–2):420–7. https://doi.org/10.1016/j.jallcom.2010.03.093.